ELSEVIER

Journal of Power Sources 62 (1996) 193–199

JOURNAL OF POWER SOURCES

Influence of cycling current and power profiles on the cycle life of lead/acid batteries

G. Papazov, D. Pavlov

Central Laboratory of Electrochemical Power Sources, Bulgarian Academy of Sciences, Sofia 1113, Bulgaria

Received 11 March 1996; accepted 2 April 1996

Abstract

Batteries are assembled with positive plates of the novel strap grid tubular (SGTP) design described in a previous paper [1]. These batteries are subjected to four tests: (i) Peukert dependence determinations; (ii) classical galvanostatic cycling (5 h charge and 1 h discharge); (iii) EV–SFUDS, and (iv) EV–ECE-15 cycling tests. It has been established that the Peukert dependence curve of SGTP batteries is very close in profile to that for SLI batteries. This guarantees SGTP's batteries high power performance. These batteries endure over 950 cycles on galvanostatic cycling. When cycled according to the SFUDS power profile under a current load of 320 A/kg positive active mass during the 15th SFUDS step, SGTP batteries exhibit a cycle life of 350–450 cycles. If the current density during the 15th step is 190 A/kg PAM, the batteries endure over 600 charge/discharge cycles. The life of positive SGT plates is limited by power loss, but not by capacity. Similar results have also been obtained from ECE-15 cycle-life tests. On cycling SGTP batteries with a current load of 210 A/kg PAM during the 23rd ECE-15 step (the step during which maximum power output is demanded from the battery), they endure between 550 and 650 charge/discharge cycles. A summary of the test results obtained for two batches of experimental batteries indicates that there is a direct dependence between the SGTP battery cycle life and the maximum current density on discharge. Increasing the discharge current density decreases the battery life. It has also been established that the capacity on SFUDS (ECE-15) discharge declines gradually on cycling in favour of the residual galvanostatic capacity at 5 h rate of discharge (100% depth-of-discharge) which increases. This implies that two types of structures are formed in the positive plates on cycling: the first type ensuring high power output and the second type yielding low power but long cycle life. The higher the power delivered by the positive plate, the faster the conversion of the structure supporting this high power output into such yielding low power performance. EV-SFUDS: A simplified version of the Federal urban driving schedule for electric vehicle battery testing, US Department of Energy, USA, 1988, and ECE-15: a standard European test cycle, speed versus time.

Keywords: Lead/acid batteries; Cycling current; Power profiles

1. Introduction

The cycle life of lead/acid batteries is often limited by the positive plates half-cell. The lead/acid battery positive plate consists of three structural elements: (i) positive active mass (PAM): (ii) corrosion layer (CL), and (iii) grid. Each of these elements may limit the life of the battery during its operation, due to certain irreversible processes that occur in the structural elements or at the interfaces between them. These processes include:

(i) *Grid corrosion.* During operation of a lead/acid battery, the positive plates have potentials at which the grid metal is thermodynamically unstable and is hence oxidized. A CL is formed between the grid and the positive active mass. This CL differs in structure and phase composition from the PAM. The process of corrosion proceeds at the grid/CL interface, as a result of which the cross section of the current collector (grid) through which the electric current flows is reduced or may even be interrupted at some places. Consequently, considerable parts of the plate are excluded from the current generation process. The capacity of the plate decreases abruptly. The battery resource is exhausted.

(ii) *Softening and shedding off of PAM.* On discharge of the battery, the PbO_2 is converted into $PbSO_4$, and the reverse process occurs on charging of the battery. These processes cause the volume of PAM to pulsate and induce changes in its skeleton structure and pore system. On cycling of the plate, certain processes occur in the agglomerates building up the skeleton of PAM, which lead to the formation of individual PbO_2 crystals [2] and to thinning of the bonds between the agglomerates [3]. As a result, the electric contacts in certain parts of PAM are impaired. Considerable zones of the PAM volume have reduced contribution to the total capacity of the plate. This process leads further to worsening of the mechan-

PII S0378-7753(96)02422-6

ical contact between the skeleton and the agglomerates, and consequently the latter shed off. The quantity of PAM which is involved in the current generation process on cycling becomes smaller and smaller leading to a gradual decline in plate capacity and power output which may reach down to the lowest allowable limit (cutoff values). The battery resource is exhausted.

(iii) *Processes at the CL/PAM interface*. The theoretical concept about the CL/PAM interface was elaborated in Ref. [1]. The interface grid/PAM consists of a CL and a thin PAM layer (active mass collecting layer, AMCL), which has the function to collect and to distribute uniformly the electric current throughout the whole PAM [1]. The smallest cross section through which the electric current passes is that at the CL/AMCL interface. The current density is the highest at this interface. Hence both the specific resistance and the cross-sectional area of the CL/PAM interface are of crucial importance for the polarization of the plate, i.e. for its capacity and power performance. The density of PAM decreases on cycling. Consequently, the area of the skeleton branches in the AMCL at its interface with the CL diminishes and the resistance of the interface increases. On discharge, a part of the PbO_2 particles in the AMCL is reduced to $PbSO_4$. Therefore, the cross section through which the current passes between PAM and the CL is further reduced and hence the degree of polarization of the plate increases. It may reach a value marking the end of discharge. Thus, the battery life is limited by the resistance of the grid/CL/PAM interface. This is the most probable mechanism of the phenomena causing the so-called premature capacity loss (PCL) [1].

Due to the great variety of applications of the lead/acid battery and especially its utilization in electric vehicles on the road, various charge and discharge current and power profiles are employed. To determine the influence of these profiles on the irreversible processes, and hence on battery cycle life, is a real challenge for researchers in the field of lead/acid batteries.

The aim of the present investigation is to study the effect of the discharge current profile on the cycle life of batteries subjected to SFUDS [1] (USA) or to ECE-15 [2] (Europe) electric vehicle (EV) cycling tests. For comparison, the same batteries are also cycled under conventional galvanostatic mode, 5 h charge followed by 1 h discharge.

2. Experimental

2.1. Possible methods to suppress the irreversible processes

Having disclosed the phenomena responsible for the PCL [1,4] we elaborated a theory about the mechanism of these processes and based on this theoretical background proposed a novel positive plate design (strap grid tubular plates, SGTP), by the use of which these phenomena were suppressed [1]. The novel positive plate is characterized by:

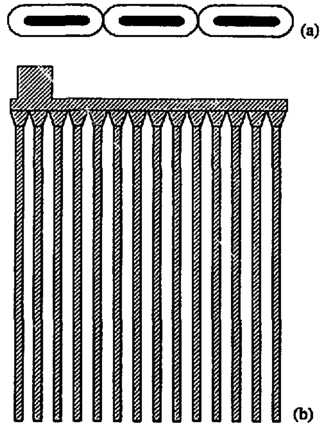

Fig. 1. A schematic representation of the strap grid tubular plate design: a) cross section, and (b) comb-like strap grid.

(i) The quantity of PAM in g per 1 cm^2 of grid area (denoted by γ coefficient) is limited to 0.8 g PAM/cm^2. A uniform PAM layer is formed on the grid surface. This is achieved by using a set of straps connected by a common top lead to form a comb-like construction instead of the conventional plate grid. The novel strap grid is presented schematically in Fig. 1(b); this design has an additional advantage. On cycling of the plate inner mechanical stresses occur between the grid and PAM. Under the action of these stresses the grid swells (creeps). This leads to cracking of the CL. With the use of the novel strap grid construction these mechanical processes are minimized.

(ii) The positive active mass is enclosed in oval tubes of woven or nonwoven polyester fabric in order to limit the pulsation of the plate and to slow down the decrease in PAM density on cycling. Each strap of the strap grid is located in the centre of the oval tube thus its surface is covered by a PAM layer of uniform thickness (1–1.5 mm) (Fig. 1(a)). This ensures uniform current density in all parts of the plate.

(iii) Tetrabasic lead sulfate (4BS) pastes are used which yield a stable PAM skeleton.

In addition to suppressing the phenomena causing PCL, the novel positive plate design has other advantages as well: (i) the rate of grid corrosion is decreased significantly: as established in Ref. [5] a 1 mm PAM layer slows down the rate of grid corrosion twice, and (ii) being enclosed in the tube volume, the PAM is safeguarded from softening and shedding.

[1] EV-SFUDS: a simplified version of the Federal urban driving schedule for electric vehicle battery testing, US Department of Eenergy, USA, 1988.
[2] ECE-15: a standard European test cycle, speed versus time.

2.2. Technology for manufacture of strap grid tubular plates (SGTP)

Strap grids were cast from Pb–1.8%Sb–0.15%As–0.2%Sn alloy. 4BS paste was prepared at 85 °C using 6% H_2SO_4 versus the leady oxide. 4BS crystals sized between 15 and 20 μm were formed in the paste. The latter was diluted with water to give a suspension with sp. gr. of 1.9–2.0. Strap grid tubular plates were filled with the suspension using a specially designed and constructed filling device. The tubes (gauntlets), produced by Amer-Sil S.A. (Luxembourg) and Tergar S.R.L. (Italy), serve as a filter for the 4BS crystals. The plates thus produced were cured for 24 h at 85 °C and then formed in H_2SO_4 sp. gr. 1.15. The formation was conducted at 520 Ah per kg PAM. These plates were assembled into 12 V batteries the capacity of which was limited only by the positive half-cell.

2.3. Testing of SGTP batteries

All battery tests were performed using BITRODE LCN cycle life testing modules:

(i) *Peukert dependence.* The specific capacity of the PAM in SGTP batteries was determined on cycling at current densities from 2 to 200 A/kg PAM.

(ii) *Capacity tests.* The capacity was determined at 5 h rate of discharge at 25 °C. The rated capacity was calculated at 50% utilization of the active mass versus the theoretical capacity.

(iii) *Battery cycle life on galvanostatic cycling.* Each cycle comprised 5 h charge at 13 mA/g PAM and 1 h discharge at 56 mA/g PAM ($Q_{discharge}/Q_{charge}=1.15$, Fig. 2). The discharge was conducted at 25% utilization of PAM versus the theoretical capacity.

(iv) *Battery cycle life on EV–SFUDS cycling.* Batteries for EV applications must meet severe demands: they must have high power and energy output and low weight at the same time. The US standard for EV-battery testing is the SFUDS test [6]. The power profile of the latter is presented schematically in Fig. 3(a).

It comprises 20 steps with different discharge, charge and rest periods. The total duration of one 20-step SFUDS cycle is 6 min. The most critical step is No. 15 during which the

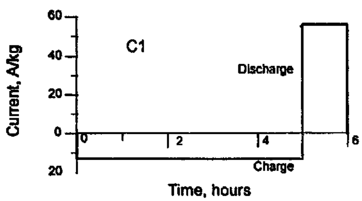

Fig. 2. Current profile of a classical galvanostatic cycle comprising 5 h charge and 1 h discharge.

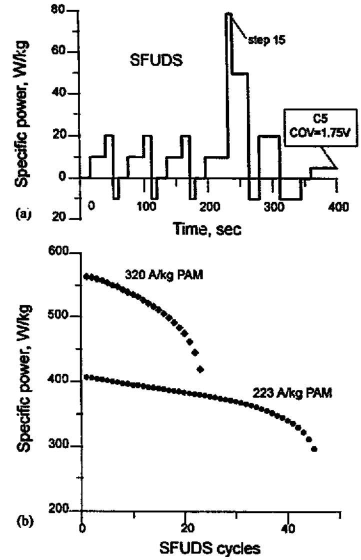

Fig. 3. EV–SFUDS cycle life test: (a) power profile of one SFUDS discharge cycle, and (b) specific power output on SFUDS battery discharge at two different current loads during the 15th SFUDS step.

battery must deliver a power of 79 W/kg for 8 s. The power demanded from the battery during the other steps is smaller.

The specific power requirements of the SFUDS test procedure refer to the specific power of the whole battery. At step No. 15 the battery should deliver 79 W/kg of battery weight. As we are interested in the behaviour of the positive plate only, the latter should be the capacity limiting element. To achieve this we used a battery with excess of negative active mass and of electrolyte to yield a capacity higher than that of the positive plate, i.e. sizing of the battery as a whole was not optimized. Hence, data about the overall battery power would not provide relevant information about the properties of the positive plate. That is why we calculated the specific power of the battery versus the weight of PAM only. In general, the latter comprises about 15% of the total battery weight. Hence, the discharge current for testing of 1 kg of positive active mass had to be 6.6 times the current per 1 kg of battery weight.

The relationship between the experimentally determined specific power and the number of SFUDS cycles (6 min each) for one battery discharge cycle is given in Fig. 3. Fig. 3(b) presents the above-mentioned dependences for the two batteries under test as a function of the number of SFUDS cycles during the first battery discharge. The tests were performed under two different current loads: 320 and 223 A/kg PAM, respectively.

As can be seen from the figure, with decreasing PAM load the delivered specific power also decreases, while the number of SFUDS cycles increases from 25 to 40–45 cycles.

On completion of each battery discharge employing the SFUDS cycles, the residual galvanostatic capacity (GC) of the batteries was determined at 5 h rate of discharge. During each cycle, the battery was first discharged using the SFUDS power profile down to a minimum power of 50 W/kg of battery weight and then the discharge was further conducted at constant current (5 h rate of discharge) down to a cutoff voltage of 1.75 V per cell. The specific energy delivered on SFUDS cycling was determined. The dependence of this specific energy on the number of charge/discharge cycles was plotted. The residual capacity (GC) as well as the capacity on SFUDS cycling (SC) were determined.

2.4. *Cycle life tests following the European ECE-15 testing procedure*

The power profile of the European ECE-15 standard for EV-battery testing is shown in Fig. 4(a). This testing procedure is much more complicated than the SFUDS test. The ECE-15 test cycle comprises two parts, an urban part with duration of 195 s which is repeated four times and a suburban part with a duration of 400 s and a maximum power requirement of 51.9 W/kg to be delivered for 24 s. The total cycle length of one ECE-15 cycle is 1180 s (about 20 min).

The results from the first ECE-15 discharge cycle under a maximum current load of 210 A/kg are presented in Fig. 4(b). The specific power of 375 W/kg PAM delivered at the beginning of cycling is very close to the power delivered on SFUDS cycling under similar current loads. The discharge capacity for one ECE-15 cycle (EC) is considerably higher than the discharge capacity for one SFUDS cycle.

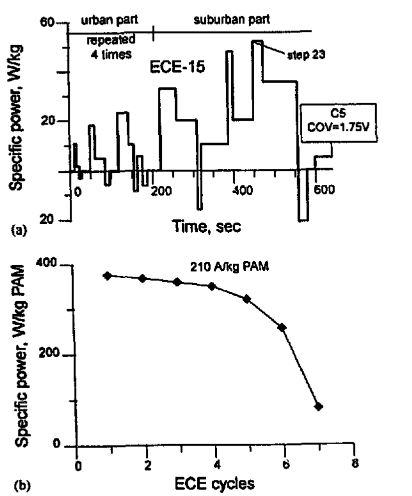

Fig. 4. EV–ECE–15 cycle life test: (a) power profile of one ECE–15 discharge cycle, and (b) specific power output on ECE–15 battery discharge at two different current loads during the 23rd ECE–15 step.

The experimental cell was subjected to cycle-life tests employing the ECE-15 discharge power profile with a maximum current load of 210 A/kg PAM. On completion of each battery discharge, the residual capacity of the battery was determined at 5 h rate of discharge (GC), so that in this test, too, the battery was actually discharged applying two discharge modes: ECE-15 (EC) and galvanostatic (GC).

3. Results

3.1. *Peukert relationship*

The relationship between the specific capacity of the positive plates (the capacity per 1 kg PAM) and the discharge current density was investigated. Three types of battery were tested: (i) SLI batteries; (ii) EV batteries with commercial positive plates, and (iii) batteries with strap grid tubular positive plates (SGTP). The obtained results are presented in Fig. 5.

The SGTP battery exhibits a specific capacity very close to that of SLI batteries and considerably higher than that of commercial EV batteries. At current loads below 55 A/kg PAM, the SGTP battery has slightly higher capacity than its SLI counterpart. At higher current densities, however, the reverse situation is observed, the specific capacity of the SLI battery is higher than that of the SGTP one. These Peukert curves indicate that SGTP batteries have a power performance close to that of SLI batteries. It is known, however, that SLI batteries have short cycle life on deep-discharge cycling. It is interesting to find out how SGTP batteries would behave on cycling and what would be their cycle life.

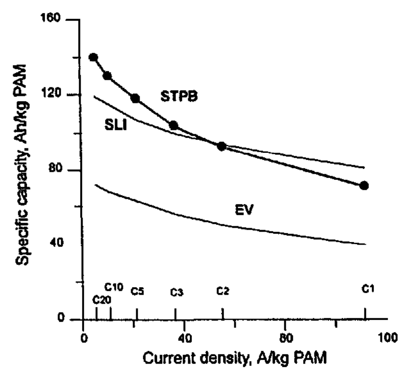

Fig. 5. Specific capacity of the positive active mass vs. discharge current density for three types of battery: SGTB: strap grid tubular plates battery; SLI: starter batteries, and EV: commercial electric vehicle battery.

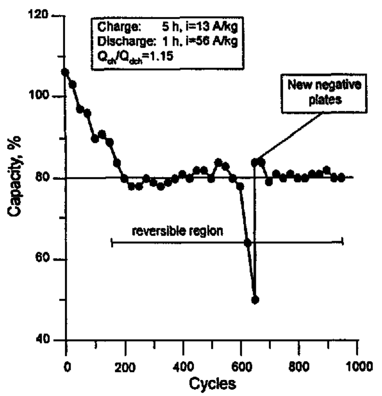

Fig. 6. Evolution of battery capacity on galvanostatic cycling: 5 h charge, 1 h discharge.

3.2. *Constant current charge/discharge cycling*

Fig. 6 presents the dependence of the capacity (in % versus the rated value) on the number of charge/discharge cycles.

A gradual capacity decrease at an average rate of 0.135% C per cycle is observed until the 200th cycle. This is a relatively low rate of capacity loss. Then, between cycles Nos. 225 and 950, the battery capacity remains almost constant and equal to about 80% of the rated value. Due to intense swelling of the negative active mass the negative half-cell was replaced with a new one after 650 cycles. The battery restored its capacity and has reached 950 cycles up to now. The cycling test is in progress.

3.3. *Cycle-life tests according to the SFUDS testing procedure*

Fig. 7 presents the experimentally determined dependence of the specific energy on the number of cycles for SLI and SGTP batteries subjected to SFUDS cycling tests. During the 15th step of the SFUDS current profile the current density was 320 A/kg PAM for the SGTP battery and 272 A/kg PAM for the SLI battery, respectively. Fig. 7(b) presents the evolution of the SFUDS capacity (SC), the residual galvanostatic capacity (GC) and the total battery capacity on cycling of SGTP batteries.

We assumed that an EV battery has reached its end of life when it fails to deliver 75 Wh/kg PAM.

The SLI battery endured only 10 cycles, while the power output of the battery with SGTP positive plates fell down to 75 Wh/kg PAM after 363 cycles. A specific peculiarity of the SFUDS test is that the specific energy/number of cycles curve declines step-wise. Each step correspond to one SFUDS cycle with specific energy output of 7.35 Wh/kg. Formally this is a kind of 'quantization' of the battery energy.

The three types of capacity exhibit interesting behaviour on cycling. During the first cycle, the total capacity of the battery is 110 Ah/kg PAM. Knowing that the theoretical capacity of 1 kg PAM is 224 Ah, it can be calculated that the utilization of PAM is 49% versus the theoretical capacity. Such an active mass utilization is typical for SLI batteries. The following capacity distribution is observed: 82% of the total capacity is utilized during the SFUDS discharge (SC) and 18% is the residual galvanostatic discharge capacity (GC).

The total capacity of the battery decreases at a fairly high rate during the first 100 cycles due to the drop in SFUDS capacity. The residual galvanostatic capacity declines but very slowly. Then between the 100th and 600th cycles, the total capacity remains almost constant and equal to 65 Ah/kg PAM or 29% utilization of PAM versus the theoretical capacity. During this period of 500 cycles the ratio between the SFUDS capacity and the residual galvanostatic capacity (SC/GC) changes. The total battery capacity at the 600th cycle is almost equal to that during the 100th cycle. According to the specific energy output demand of the SFUDS test, the battery must have reached its end of life already after 363 cycles. However, the total capacity indicates that it is still in good health after 600 cycles.

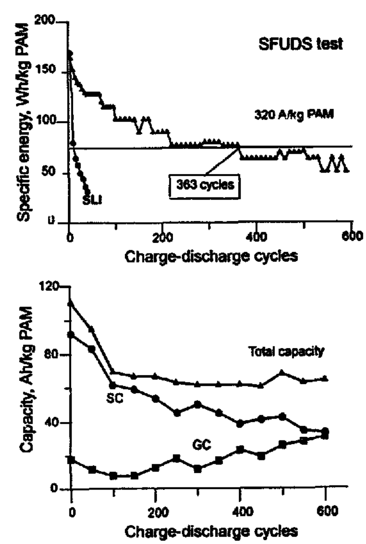

Fig. 7. Changes in specific energy and in the three types of capacity on SFUDS cycling: current density during the 15th SFUDS step was 320 A/kg PAM. SC: capacity on SFUDS discharge, and GC: residual capacity at 5 h rate of discharge (100% depth-of-discharge).

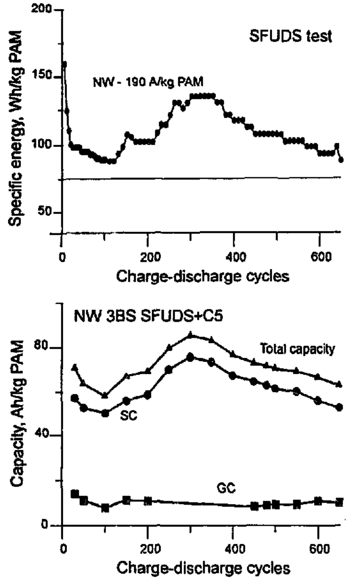

Fig. 8. Changes in specific energy and in the three types of capacity on SFUDS cycling: current density during the 15th SFUDS step was 190 A/kg PAM.

The above-mentioned behaviour of the specific energy and the total battery capacity suggests that there is a phenomenon that determines the life of the battery, namely the existence of two types of capacity: (i) one ensuring battery discharge at high power output (SC), and (ii) one being the residual capacity at low power discharge (GC). During battery operation the ratio between these two types of capacity changes, the GC increasing at the expense of the SC.

Fig. 8 presents the results from SFUDS testing of an SGTP battery under a current load of 190 A/kg PAM during the 15th SFUDS step.

The specific energy/number of cycles curve (Fig. 8(a)) features a minimum and a maximum. The battery preserves its capacity above 75 Wh/kg for over 650 cycles. Tests are going on. The SC follows, quite naturally, the profile of the specific capacity/number of cycles curve. The residual galvanostatic capacity (GC) preserves a constant value throughout the battery cycle life. Hence, the total battery capacity also follows the SC profile.

On comparing the data in Figs. 7 and 8, it becomes evident that the cycle life of batteries cycled according to the SFUDS EV battery testing procedure depends very strongly on the current density during the 15th SFUDS step. The battery life increases at lower current densities.

3.4. Cycle-life tests according to the ECE-15 testing procedure

Battery tests were performed according to the ECE-15 standard for EV battery testing at a current load of 210 A/kg PAM during the 23rd step of the ECE-15 profile. The obtained results are presented in Fig. 9.

The specific energy delivered by PAM fell down below 75 Wh/kg after 562 cycles. Up to the 225th cycle, the specific energy output declined gradually and maintained an almost constant value between the 225th and the 562nd cycles.

In this case, too, the total battery capacity marks a gradual decrease during the first 250 cycles and remains almost unchanged thereafter until 625 cycles are completed. Here again the total battery capacity is preserved, the ratio between the ECE discharge capacity (EC) ensuring discharge with high power output and the residual galvanostatic capacity (GC) at 5 h rate of discharge is changed in favour of the latter.

3.5. Battery cycle life as a function of current density

Fig. 10 shows the number of cycles endured by two series of battery under test as depending on (i) the maximum discharge current density on SFUDS and ECE-15 cycling and

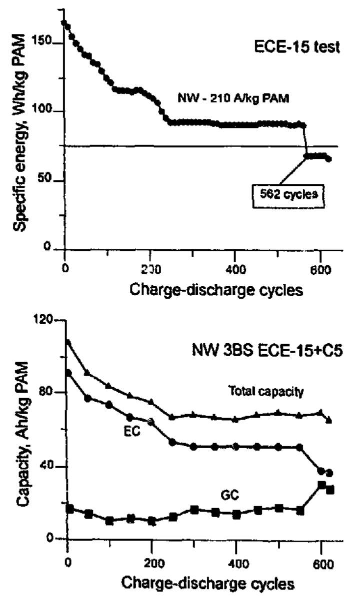

Fig. 9. Changes in specific energy and in the three types of capacity on ECE-15 cycling: current density during the 23rd ECE-15 step was 210 A/kg PAM.

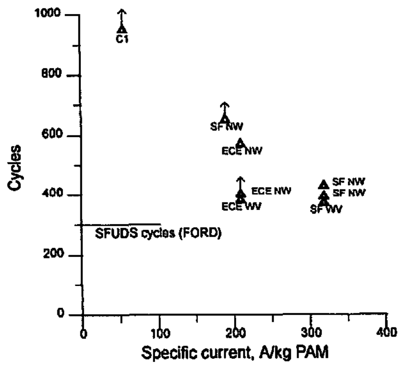

Fig. 10. Battery cycle life as a function of the maximum current load for the three types of cycling test.

(ii) on the current density during the 1 h galvanostatic discharge. The test results for eight batteries are summarized.

The following conclusions can be drawn from the figure:

(i) The maximum discharge current density applied, though only for a short period (an impulse of 8 s), exerts an almost limiting influence on the cycle life of positive strap grid tubular plates. The higher the current density on discharge, the shorter is the life of the battery.

(ii) The above-mentioned tests were performed employing three different current profiles. Nevertheless, the current density/number of cycles dependence tends towards a straight line. However, the relatively small number of batteries tested up to now does not allow to make a definite statement that such a linear relationship exists. Further investigations are needed to verify these initial results.

(iii) The batteries produced with positive plates of the novel strap grid tubular design and the newly developed technology exhibit high cycle life performance, which is an unequivocal evidence of the correctness of the theoretical assumptions on which the new design was based [1].

4. Conclusions

The results discussed above indicate that the novel strap grid tubular plate design is characterized by both high power and energy performance, and long cycle life, and would therefore meet well the EV battery requirements in particular the demands of the SFUDS and the ECE-15 standards. Both SFUDS and ECE-15 cycling tests include steps demanding high power output. The structure of the plates is altered as their SFUDS (ECE) capacity and energy performance decline, and so does their cycle life. The capacity of the plates at 5 h rate of discharge does not change substantially at that. This power loss is a result of certain processes that lead to changes in the structure of the plate as a result of which its inner resistance increases and hence the battery power output declines. These structural changes will be the subject of another paper to follow.

Acknowledgements

The authors acknowledge with gratitude the financial support provided by The Advanced Lead Acid Battery Consortium, a Program of The International Lead Zinc Research Organization, Inc., NC, USA, for implementation of the present research.

References

[1] D. Pavlov, *J. Power Sources, 53* (1995) 9.

[2] J. Yamashita, H. Yufu and Y. Matsumaru, *J. Power Sources, 30* (1990) 13.

[3] A. Winsel, E. Voss and U. Hullmeine, *J. Power Sources, 30* (1990) 209.

[4] D. Pavlov, *J. Power Sources, 48* (1994) 179.

[5] T. Rogachev, G. Papazov and D. Pavlov, *J. Power Sources, 10* (1983) 291.

[6] EHP Battery test Working Task Force, USA, Department of Energy, Rep. No. *DOE/ID-10146*, Aug. 1988.